

# Range Retrieval with Graph-Based Indices

Magdalen Dobson Manohar  
Carnegie Mellon University and  
Microsoft Azure  
USA  
mmanohar@microsoft.com

Taekseung Kim  
Carnegie Mellon University  
USA  
taekseuk@andrew.cmu.edu

Guy E. Blelloch  
Carnegie Mellon University and  
Google  
USA  
guyb@cs.cmu.edu

## Abstract

Retrieving points based on proximity in a high-dimensional vector space is a crucial step in information retrieval applications. The approximate nearest neighbor search (ANNS) problem, which identifies the  $k$  nearest neighbors for a query (approximately, since exactly is hard), has been extensively studied in recent years. However, comparatively little attention has been paid to the related problem of finding all points within a given distance of a query, the *range retrieval* problem, despite its applications in areas such as duplicate detection, plagiarism checking, and facial recognition. In this paper, we present a set of algorithms for range retrieval on graph-based vector indices, which are known to achieve excellent performance on ANNS queries. Since a range query may have anywhere from no matching results to thousands of matching results in the database, we introduce a set of range retrieval algorithms based on modifications of the standard graph search that adapt to terminate quickly on queries in the former group, and to put more resources into finding results for the latter group. Due to the lack of existing benchmarks for range retrieval, we also undertake a comprehensive study of range characteristics of existing embedding datasets, and select a suitable range retrieval radius for eight existing datasets with up to 100 million points in addition to the one existing benchmark. We test our algorithms on these datasets, and find up to 100x improvement in query throughput over a naive baseline approach, with 5-10x improvement on average, and strong performance up to 100 million data points.

## 1 Introduction

Similarity search within databases of high-dimensional vectors has become increasingly important over the last decade due to the rise of semantic embeddings generated by neural networks and large language models (LLMs). Similarity search is a foundational building block of applications such as search, recommendations, advertising, and retrieval augmented generation (RAG). Correspondingly, there has been an explosion of work on efficient algorithms for approximate similarity search [8, 12, 15, 23], as exact similarity search is prohibitively expensive due to the curse of dimensionality.

The object of approximate similarity search, or approximate nearest neighbor search (ANNS) is finding the top- $k$  most similar embeddings. These top- $k$  results can then be post-processed for the desired application. However, there are some applications for which retrieving top- $k$  embeddings for a fixed  $k$  is a poor fit. Applications such as duplicate detection, plagiarism checking, and facial recognition require instead to retrieve all results within a certain *radius* of a query rather than top- $k$ , with some post-processing after to verify whether a match exists out of the retrieved items [7, 18, 20]. Furthermore, in real-world search applications some queries may have tens of thousands of matches while others have none or very

few. In these cases, search with a small radius, or range retrieval, may be used to both differentiate these query types [24]. Range search can also be a useful subroutine in applications using nearest neighbor graphs, such as clustering or graph learning [10, 14].

Range search differs from top- $k$  search by the diversity in size of the ground truth solutions for a set of queries. In practice, solutions for a set of queries follow a skewed, Pareto-like distribution where the majority of queries tend to have no results within the chosen radius, while a smaller fraction have a small number of results, and a few outliers have thousands to tens of thousands of results. Queries in the middle category are well served by existing similarity search algorithms, which are already highly optimized and efficient. Thus, a good range search algorithm will match the efficiency of top- $k$  search on the middle category of queries, while quickly terminating on queries with no results, and efficiently finding all results for those few queries with thousands of results.

Despite the many applications of range search, there has been very little work on designing algorithms specifically for the task of high-dimensional range search. From a practical perspective, it would be ideal if data structures for top- $k$  search could be reused or lightly adapted for range search, enabling an existing data structure to serve both types of queries. Data structures for top- $k$  search typically fall into one of two categories—partition-based indices, which partition the dataset into cells and exhaustively search a small number of cells at query time, and graph-based indices, which construct a proximity graph over the data points and use a variant of greedy search to answer queries. Graph-based indices are widely acknowledged as achieving equal or better similarity search performance than partition-based indices [27], but almost no work has studied the question of adapting graph-based indices for range retrieval. Furthermore, top- $k$  search with IVF indices naturally explores thousands of candidates per query by exhaustively checking the distances between the query point and all the points in each cell, while the number of nodes a graph-based search typically explores is only a small multiple of  $k$ . It is thus a much less trivial algorithmic task to adapt graph-based search to serve such queries (as we will show in Section 4, naive adaptations of existing search methods are not adequate for the task). The graph structure also suggests potential to terminate queries with no results after examining just a handful of vertices. It is natural then to ask whether graph-based indices can be adapted to efficiently serve range queries.

*Our Contributions* In this paper, we present a set of algorithms designed for approximate high-dimensional range search on graph-based ANNS indices. Our techniques are modifications of the standard graph search algorithm, meaning that we enable one data structure to efficiently serve both top- $k$  queries and range queries. We present techniques that allow a range query to quickly terminate when the query has no results, and to efficiently answer

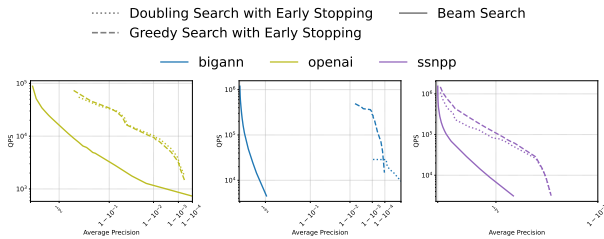


**Figure 1: A preview of our experimental results on three datasets: from left to right, OpenAI-1M, BIGANN-10M, and SSNPP-100M. The solid line shows the beam search baseline, while the dotted and dashed lines show our two new algorithms. Datasets and algorithms are described in detail in Sections 3 and 4, respectively.**

queries with thousands of results within their radius. We devise an early-stopping heuristic that is capable of predicting whether a query has no results after only a few hops in the graph search. For queries with many results, we design two algorithms, *doubling search* and *greedy search*, that extend the search path to return more results while minimizing wasted work, and compare and contrast situations where each algorithm dominates the other.

For our experimental evaluation, since there is only one publicly released dataset specifically for range search, we evaluate eight state-of-the-art publicly available metric embedding datasets with up to 100 million embeddings and select a suitable radius for each one. We also perform additional analysis of the characteristics of different range search datasets, and how they connect to the magnitude of improvement our algorithms achieve.

We evaluate our algorithms on the set of nine datasets (eight contributed by us, and one public benchmark), and find that our range retrieval algorithms are capable of up to 100x speedup over naive adaptations of top- $k$  search, and in most cases 5-10x speedup. We additionally find that the speedup and scalability of our algorithms extends up to datasets with 100 million points. Figure 1 shows a preview of our experimental results on three embedding datasets of sizes one million to 100 million. In each case, for a fixed average precision, we find at least a 10x speedup in throughput; additionally, our algorithms extend to significantly higher accuracy than the baseline.

*Outline* In Section 1.1 we cover related work. In Section 2 we cover some needed preliminaries. In Section 3 we explore the characteristics of range search datasets and provide heuristics for choosing an acceptable radius, which we use to adapt eight public embedding datasets for range searching. In Section 4 we present our algorithms for range search on graph-based indices, and in Section 5 we present experimental results.

## 1.1 Related Work

*Work on Range Searching* Some earlier work addresses range retrieval in high dimensions from a theoretical standpoint [4], or with only minimal experiments that do not extend to the large embeddings used today [25]. Theory results on nearest neighbor search using locality sensitive hashing (LSH) also implicitly apply to range search, since their approximation guarantees are usually in the form of finding neighbors within a  $(1 + \epsilon)$  radius of the distance to the true top- $k$  result [11].

On the practical side, Meta AI released a range retrieval dataset aimed towards detecting misinformation [18], which was used as one of the competition datasets in the NeurIPS 2021 Big ANN Benchmarks Challenge [22], but competitors solved this task using naive adaptations of top- $k$  search rather than novel range searching algorithms. A recent work by Szilvasy, Mazare, and Douze [24] addresses the combined task of retrieving range search results with one metric and then re-ranking them using a more sophisticated model. They address the question of designing a range search metric (RSM) specifically for *bulk* search—that is, range search over a group of queries with a fixed computational budget—and benchmark its results on an image search application. They use an inverted file (IVF) index, a common data structure for similarity search [6], to serve their database queries.

The Starling system [26] is an SSD-resident graph-based ANNS index optimized for I/O efficiency. Their work includes benchmarks on range search metrics, and they use an algorithm similar to the doubling beam search algorithm we present in Section 4. However, the focus of their paper is not on comprehensive benchmarking of range search, and since their implementation is a disk-resident index and ours is fully in-memory, our experiments are not directly comparable to theirs.

*Other Related Work* Some variants on the high-level ideas behind our range search algorithms—that is, early termination of queries with few results, and extensions of beam search for queries with many results—have been used before in the context of nearest neighbor search. A work by Li et al. [13] uses a machine learning model to predict when a query can terminate early and still maintain high accuracy. Another work [28] uses graph search with two phases (essentially, an initial cheaper phase and a later, more compute intensive phase for selected queries to gather additional candidates).

## 2 Preliminaries

Here, we define the range search problem and the metric for measuring the accuracy of the search. Range searching, conceptually, can be defined as retrieving results within a ball of radius  $r$  for a given metric space. We then define average precision, which indicates how well a search algorithm finds the correct result given a set of queries.

In this work, we study a set  $\mathcal{P} \subseteq \mathbb{R}^d$  of  $n$  points (vectors) in  $d$  dimensions. We denote the *distance* between two points  $p, q \in \mathbb{R}^d$  as  $\|p, q\|$ . Smaller distance indicates greater similarity.

Commonly-used distance functions include Euclidean distance ( $L_2$  norm), and maximum inner product search, which uses negative inner product as a distance function.

**Definition 2.1** (Range Search). Given a set of points  $\mathcal{P}$  in  $d$ -dimensions, a query point  $q$  and radius  $r$ , the range search problem finds a set  $\mathcal{K} \subseteq \mathcal{P}$  such that  $\max_{p \in \mathcal{K}} \|p, q\| \leq r$ .

Next we define average precision, a commonly used metric that captures the accuracy of a search algorithm. Note that the measure weights a point’s contribution to average precision proportionately to its size.

**Definition 2.2** (Average Precision). Let  $\mathcal{P}$  be a set of points in  $d$ -dimensions and  $Q$  a query point set. For  $q \in Q$ , let  $\mathcal{K}$  be the true

range neighbors of  $q$  in  $\mathcal{P}$ . Let  $\mathcal{K}' \subset \mathcal{P}$  be an output of a range search algorithm. Then *Average Precision* is defined as  $\frac{\sum_{q \in Q} |\mathcal{K} \cap \mathcal{K}'|}{\sum_{q \in Q} |\mathcal{K}'|}$

### 3 Characteristics of Range Search Datasets

In this section, we take eight existing embedding datasets from top- $k$  retrieval benchmarks and show how to use them for range search—namely, by finding a radius which yields a suitable distribution. We evaluate the characteristics of each dataset; alongside, we also evaluate the one existing range search benchmark.

For a dataset to be meaningful as a range search benchmark, the same distance  $\epsilon$  must be indicative of a match for each query point. While this is not necessarily the case for all embedding datasets, it is not directly observable without full access to the source material, and even with that access would be incredibly costly to determine. Thus, we use the characteristics of existing benchmarks to determine whether a dataset is suitable, and select a radius if so. Real-world query sets tend to follow a power-law distribution, where most points have no matches, while a handful of points have thousands of matches [18, 24]. To be useful as a range search benchmark, a query set should roughly follow this distribution in the number of matches for each query.

Another important aspect of suitability for range search is whether there exists a choice of radius that is “robust” in the sense that small perturbations of the radius do not result in a wildly different match distribution. Our later experiments show that datasets that are more robust by this measure tend to perform better over the baseline measures than ones which are more easily perturbed.

See Figure 2 for a description of each dataset used in our benchmarks.

#### 3.1 Density of Matches by Dataset

We begin our investigation by computing a measure of density of each dataset, in order to both find a suitable radius and determine whether the choice of radius is “robust” in the sense that small changes to the radius do not result in drastically more points in each ball around a query point. To do this, we take each dataset and vary the radius, recording what we refer to as the “percent captured” for each radius—that is, for each query point  $q$  and radius  $r$ , what fraction of the dataset is captured in the ball of radius  $r$  around  $q$ ?

This information is presented for each dataset in Figure 3, which shows Euclidean and inner product datasets separately and plots the percent captured from the largest radius achieving 0% capture to the smallest radius achieving 100% capture. As shown in the figure, there is wide variation in each dataset’s response to perturbations in the radius. Datasets BIGANN, GIST, DEEP, Wikipedia, and MSMARCO are the most robust to perturbations in the interesting range (for million size datasets, the applicable range is around  $10^{-6}$  to  $10^{-5}$ , as most query points will have no results). In these datasets, it is thus less likely that there will be significant numbers of points near the boundary of the ball of radius  $r$ , and thus less work to distinguish points that are just inside the boundary from those which are just outside the boundary. We will see this insight at work in the experimental results in Section 5.

Using the insights from this experiment, we choose an appropriate radius for each dataset. The real (non-normalized) choices for

each radius are shown in Figure 2.

#### 3.2 Frequency Distribution of Matches

Given a choice of radius for each dataset, we now evaluate the frequency distribution of the number of range results for each query point. The distributions are found in Figure 4. We observe a general pattern of most queries having no results and a few large outliers, which is more pronounced in BIGANN, DEEP, MSTuring, and Text2Image, and less pronounced in SSNPP, OpenAI, Wikipedia, and MSMARCO. GIST is unusual among the datasets in having many extremely large outliers. For BIGANN, SSNPP, and Wikipedia, we also show the frequency distribution for a larger version of the same base dataset. Since these are effectively larger samples from the same distribution, we observe an increase in density of range results.

### 4 Algorithms for Range Search on Graph-Based ANNS Indices

In this section we introduce our range search algorithms. We first introduce the data structure and baseline algorithm, a standard beam search. Since the standard beam search is well known to produce excellent results for top- $k$  queries, some range queries (those with an intermediate number of results) can already be efficiently answered with top- $k$  search with a small  $k$ . Thus, in this section we focus on improving queries outside this range, both queries with many results and queries with no results. Intuitively, both types of queries call for some dynamic adjustments to the beam search: for queries with no results, ideally terminating quickly before the end of the search, and for queries with many results, dynamically extending the size of the beam in some way.

#### 4.1 Data Structure and Baseline Algorithm

As the aim of this paper is to investigate whether ANNS graphs can be effectively reused for range search, the data structure used for range queries is an ANNS graph. There are many examples of ANNS graphs in the literature [8, 15, 23]. For the experiments in this paper we use the in-memory construction of DiskANN, specifically the ParlayANN library [16], but the algorithms we present should work on any single-layer ANNS graph that performs well using the standard beam search, and should be modifiable to multi-layer graphs such as HNSW with little effort.

For our baseline algorithm, due to lack of existing algorithms for range search in high dimensions, we use standard beam search on an ANNS graph. This algorithm is described in detail in many publications, and we also show pseudocode in Algorithm 1.

#### 4.2 Improving Range Search for Queries with Many Results

We first investigate how to approach graph-based range search for queries that have many results. A standard beam search can only capture as many points as are contained within the beam of size  $B$ , and thus any queries with significantly more than  $B$  results cannot achieve high accuracy. The natural question is whether it is possible to distinguish between such queries with more than  $B$  results and expand the set of returned candidates for those queries, without wasting time on queries with fewer than  $B$  results. In this section we discuss two algorithmic approaches to this idea.

Dataset	Metric	Dimension	Query Size	Selected Radius	Source
BIGANN	L2	128 (uint8)	10000	10000	SIFT descriptors of images [12]
DEEP	L2	96 (float)	10000	.02	Image embeddings from the last fully-connected layer of the GoogLeNet model [3]
MSTuring	L2	100 (float)	100000	.3	Bing queries encoded by Turing AGI v5 [29]
GIST	L2	968 (float)	10000	.5	GIST descriptors of images [12]
SSNPP	L2	200 (uint8)	100000	96237	SimSearchNet++ encodings of images [18]
OpenAI	L2	1536 (float)	10000	.2	ArXiv articles embedded using the OpenAI text-embedding-ada-002 model [9]
Text2Image	IP	200 (float)	100000	-.6	Image embeddings produced by the Se-ResNext-101 model [3]
Wikipedia	IP	768 (float)	5000	-10.5	Wikipedia articles embedded from the cohere.ai multilingual 22-12 model [19]
MSMARCO	IP	768 (float)	9374	-62	Clicked document-query pairs from the ClueWeb22 website corpus [5]

Figure 2: Descriptions of each dataset used in our experiments, along with the radius used for range search. Every dataset is publicly available [2, 21]. The SSNPP dataset is a range search benchmark, while the other datasets were originally published as top- $k$  benchmarks.

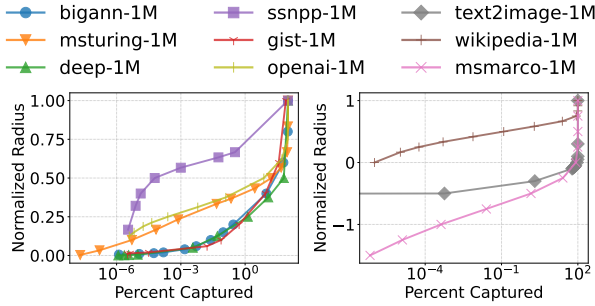


Figure 3: Plots of radius versus percent captured for each dataset: Euclidean datasets on the left and inner product datasets on the right. Radius is normalized to enable displaying multiple datasets on one plot. Note that inner product values can be less than zero, so negative ranges of radius are present on the right-hand figure.

Dataset	0	$\leq 10^1$	$\leq 10^2$	$\leq 10^3$	$\leq 10^4$	$\leq 10^5$
BIGANN-1M	9728	143	84	45	0	0
BIGANN-10M	9590	173	99	93	45	0
BIGANN-100M	9413	212	136	101	93	45
DEEP-1M	9923	56	19	2	0	0
MSTuring-1M	95716	2443	20	21	0	0
GIST-1M	8487	830	160	143	134	246
SSNPP-1M	97422	2424	254	0	0	0
SSNPP-10M	91575	7310	954	161	0	0
SSNPP-100M	80795	13719	4357	971	158	0
OpenAI-1M	7030	2564	372	34	0	0
Text2Image-1M	99327	669	4	0	0	0
Wikipedia-1M	4445	482	73	0	0	0
Wikipedia-10M	3385	1328	277	10	0	0
MSMARCO-1M	7022	2199	152	3	0	0

Figure 4: Table showing the distribution of result sizes for each dataset. Note that not all datasets have the same number of query points; see Figure 2 for the number of queries and corresponding radius for each dataset. No data point had more than  $10^5$  results.

*Doubling Beam Search* The first, and perhaps most natural, algorithm extending beam search to queries with variable number results is a dynamic beam search: that is, run the beam search with some starting beam  $B$  for a certain number of steps, then either terminate or double the beam and continue searching for more candidates. The algorithm terminates if fewer than some fraction  $\lambda$  of returned candidates are valid range candidates, and continues otherwise. In practice, we found that the value of  $\lambda$  did not change the results very much, so we set it to 1 as a rule. That algorithm is shown using beam search as a subroutine in Algorithm 5.

**Algorithm 1:** BeamSearch( $q, G, \mathcal{P}, S, r, b, \mathcal{M}$ ).

**Input:** Query point  $q$ , graph  $G$ , point set  $\mathcal{P}$ , starting points  $S$ , radius  $r$ , beam size  $b$ , early stopping metric  $\mathcal{M}$   
**Output:** Set  $\mathcal{B}$  of closest points, set  $\mathcal{V}$  of visited points

```

1  $\mathcal{B} \leftarrow S, \mathcal{V} \leftarrow \emptyset$ 
2 while  $\mathcal{B} \setminus \mathcal{V} \neq \emptyset$  do
3    $p^* \leftarrow \arg \min_{(p \in \mathcal{B} \setminus \mathcal{V})} \|p, q\|$ 
4   // Early stopping conditions
5   if  $\mathcal{M}(q, \mathcal{B}, \mathcal{V}, r)$  then Break
6    $\mathcal{V} \leftarrow \mathcal{V} \cup \{p^*\}$ 
7    $\mathcal{B} \leftarrow \mathcal{B} \cup (N_{out}(p^*) \setminus \mathcal{V})$ 
8   if  $|\mathcal{B}| > b$  then trim  $\mathcal{B}$  to size  $b$ , keeping the closest points to  $q$ 
9 return  $(\mathcal{B}, \mathcal{V})$ 

```

**Algorithm 2:** GreedySearch( $q, G, \mathcal{P}, S, r$ ).

**Input:** Query point  $q$ , graph  $G$ , point set  $\mathcal{P}$ , starting points  $S$ , radius  $r$   
**Output:** Set  $\mathcal{V}$  of visited points

```

1  $\mathcal{F} \leftarrow S, \mathcal{V} \leftarrow \emptyset$ 
2 while  $\mathcal{F} \setminus \mathcal{V} \neq \emptyset$  do
3    $p^* \leftarrow \arg \min_{(p \in \mathcal{F} \setminus \mathcal{V})} \|p, q\|$ 
4    $\mathcal{V} \leftarrow \mathcal{V} \cup \{p^*\}$ 
5   foreach  $f \in (N_{out}(p^*) \setminus \mathcal{V})$  do
6     if  $\|f, q\| \leq r$  then  $\mathcal{F} = \mathcal{F} \cup \{f\}$ 
7 return  $\mathcal{V}$ 

```

**Algorithm 3:** EarlyStopping( $q, \mathcal{B}, \mathcal{V}, \mathcal{M}, C$ ).

**Input:** Query point  $q$ , current beam  $\mathcal{B}$ , visited set  $\mathcal{V}$ , early stopping metric  $\mathcal{M}$ , cutoff parameter set  $C$   
**Output:** Bool value for early stopping. True if conditions are met.

```

1 if  $\mathcal{M}(q, \mathcal{B}, \mathcal{V}, C)$  then return True

```

**Algorithm 4:** EarlyStoppingExample( $q, \mathcal{B}, \mathcal{V}, v, C = \{r, vl, esr\}$ ).

**Input:** Query point  $q$ , current beam  $\mathcal{B}$ , visited set  $\mathcal{V}$ , number of visited points  $v$ , radius  $r$ , limit of number of visits  $vl$ , early stopping radius  $esr$   
**Output:** Bool value for early stopping.

```

// When the closest point in the beam is not within the radius
1 return  $(\arg \min_{p \in \mathcal{B}} \|p, q\| > r, \text{ and}$ 
// When the number of visited points is larger than the given cutoff
2    $v \geq vl, \text{ and}$ 
// When the current point visited is not within the early stopping radius
3    $\arg \min_{p^* \in \mathcal{V} \setminus \mathcal{B}} \|p^*, q\| > esr)$ 

```

*Greedy Search* Another approach to dynamically resizing the queue length is to run a beam search with *unbounded* queue length,

**Algorithm 5:** DoublingSearch( $q, G, \mathcal{P}, S, r, b, \mathcal{M}$ ).

**Input:** Query point  $q$ , graph  $G$ , point set  $\mathcal{P}$ , starting points  $S$ , radius  $r$ , beam size  $b$ , early stopping metric  $\mathcal{M}$

**Output:** Set of neighbors  $\mathcal{N}$  within range

```

1 while true do
2    $\mathcal{N} \leftarrow \emptyset$ 
3   // Early stopping is done inside the beam search
4    $(\mathcal{B}, \mathcal{V}) \leftarrow \text{BeamSearch}(q, G, \mathcal{P}, S, r, \mathcal{M}, b)$ 
5    $S \leftarrow S \cup \mathcal{V}$ 
6   for  $n \in \mathcal{B}$  do
7     if  $\|n, q\| \leq r$  then  $\mathcal{N} = \mathcal{N} \cup \{n\}$ 
8   if  $|\mathcal{N}| < b$  then Break
9    $b \leftarrow 2 \times b$ 
10 return  $\mathcal{N}$ 

```

**Algorithm 6:** GreedyRangeSearch( $Q, G, \mathcal{P}, S, r, b, \mathcal{M}$ ).

**Input:** Query points  $Q$ , graph  $G$ , point set  $\mathcal{P}$ , starting points  $S$ , radius  $r$ , beam size  $b$ , early stopping metric  $\mathcal{M}$

**Output:** Set of neighbors  $\mathcal{V}$  within range for each of the query points

```

1 parallel for  $q \in Q$  do
2    $\mathcal{N} \leftarrow \emptyset$ 
3    $(\mathcal{B}, \mathcal{V}) \leftarrow \text{BeamSearch}(q, G, \mathcal{P}, S, r, b, \mathcal{M})$ 
4   // Early stopping is done inside the beam search
5   foreach  $n \in \mathcal{B}$  do
6     if  $\|n, q\| \leq r$  then  $\mathcal{N} = \mathcal{N} \cup \{n\}$ 
7   if  $|\mathcal{N}| < b$  then  $\mathcal{V}[q] \leftarrow \mathcal{N}$ 
8   else
9     // Add results from beam search as starting points for greedy search
10     $\mathcal{V}[q] \leftarrow \text{GreedySearch}(Q, G, \mathcal{P}, \mathcal{N}, r)$ 
11 return  $\mathcal{V}$ 

```

but much stricter criteria on which nodes are explored. In this approach, candidates are first generated by an initial beam search with beam  $B$ . If the number of candidates within the radius falls above a certain threshold (again, some fraction  $\lambda$  of the candidates returned, which we found in practice not to matter significantly), the search moves onto this so-called "greedy search," which has an unbounded queue but only adds nodes to the queue if they are within the ball of radius  $r$  around the query point for the specified radius. This approach takes advantage of the fact that nodes in the same ball of radius  $r$  are likely to be in connected clusters, and avoids the overhead of the doubling beam search by performing very few distance comparisons to points which are not valid results. See Algorithm 2 for a complete description, and Section 5 for experimental analysis.

### 4.3 Improving Range Search for Queries with No Results

This section introduces an algorithm which improves range search for queries with no results. We start from the established paradigm of starting a search with fixed beam  $B$  and continuing with Algorithm 2 or Algorithm 5 if the returned list contains only candidates within the radius. It would be ideal to terminate the initial beam search early if the query is not finding any results, and the termination condition should use terms that are already computed during the beam search, or inexpensive to compute. A 2020 paper from Li, Zhang, Anderson, and He [13] addresses a similar question—finding conditions for terminating top- $k$  search

early—and finds that several existing terms can be used to predict whether a search can terminate early. Those terms included the coordinates of the query point, the distance from the query point to the current top- $k$  neighbor for fixed  $k$ , and the ratio of the distance from the query point to top- $k$  neighbor and the distance from the query point to the start node.

To apply these ideas to range search, the key question is whether any of these metrics are effective at distinguishing queries with zero results from queries with one or more results. To investigate this, we look at each dataset and separate each query set into three groups: those with no results, those with 1-2 results, and those with more than three results. Then, we histogram the values of these metrics at different steps in the beam search, distinguishing between these three groups. We evaluate the following metrics, the last three of which are proposed in [13].

- $d_{\text{visited}}$ : distance from query point  $q$  to the point being visited at step  $i$  of a beam search.
- $d_{\text{top1}}$ : distance from query point  $q$  to the closest known neighbor of  $q$  at step  $i$  of a beam search.
- $d_{\text{top10}}$ : distance from query point  $q$  to the tenth-closest known neighbor at step  $i$  of a beam search.
- $d_{\text{top10}}/d_{\text{start}}$ : ratio of  $d_{\text{top10}}$  to the distance from query point  $q$  to the starting point of the beam search.

Figure 5a histograms the metrics above for MSMARCO-1M at step 20 of a beam search with beam 100. Algorithm 3 shows a natural and general algorithm for imposing an early stopping condition on range search, using any one of these metrics. In all cases, when a search has already found at least one candidate within the specified range, the search does not terminate early. Otherwise, the early stopping condition is applied after a certain number of steps in the beam search. The algorithm terminates when the chosen metric is above a pre-specified cutoff. Thus, in Figure 5a, we show the same histograms as in Figure 5b, with points where the search has already found a point inside the radius excluded. The figure also shows vertical lines indicating a potential cutoff for Algorithm 3; points with more than one range result to the right of the line would be "incorrectly" cut off from further search, while points with zero points to the right of the line would be "incorrectly" allowed to proceed instead of terminating early. The goal is to identify a cutoff that yields a more favorable QPS/recall curve. Figure 5c shows one choice of metric— $d_{\text{visited}}$  on four different datasets.

Based on this data, a larger set of which is shown in Appendix A, we come to three conclusions: first, some datasets show potential for significant improvement using early stopping, while others do not. Second, if a dataset shows potential for improvement using one metric, it also tends to show improvement for all other metrics. Third, using  $d_{\text{visited}}$  seems to be the best early stopping metric, when examined using the exclusion criteria in Figure 5b. We hypothesize that  $d_{\text{visited}}$  is the best metric as it is the most frequently updated and contains the most granular information, but the positive results from other metrics suggests that approaches using machine learning such as those in the Li et al. paper [13] might also be useful. We present experimental analysis of this algorithm in Section 5. See Algorithm 4 for an example of how to apply the  $d_{\text{visited}}$  metric during a search, and Algorithm 6 for an example of the end-to-end algorithm using greedy search.

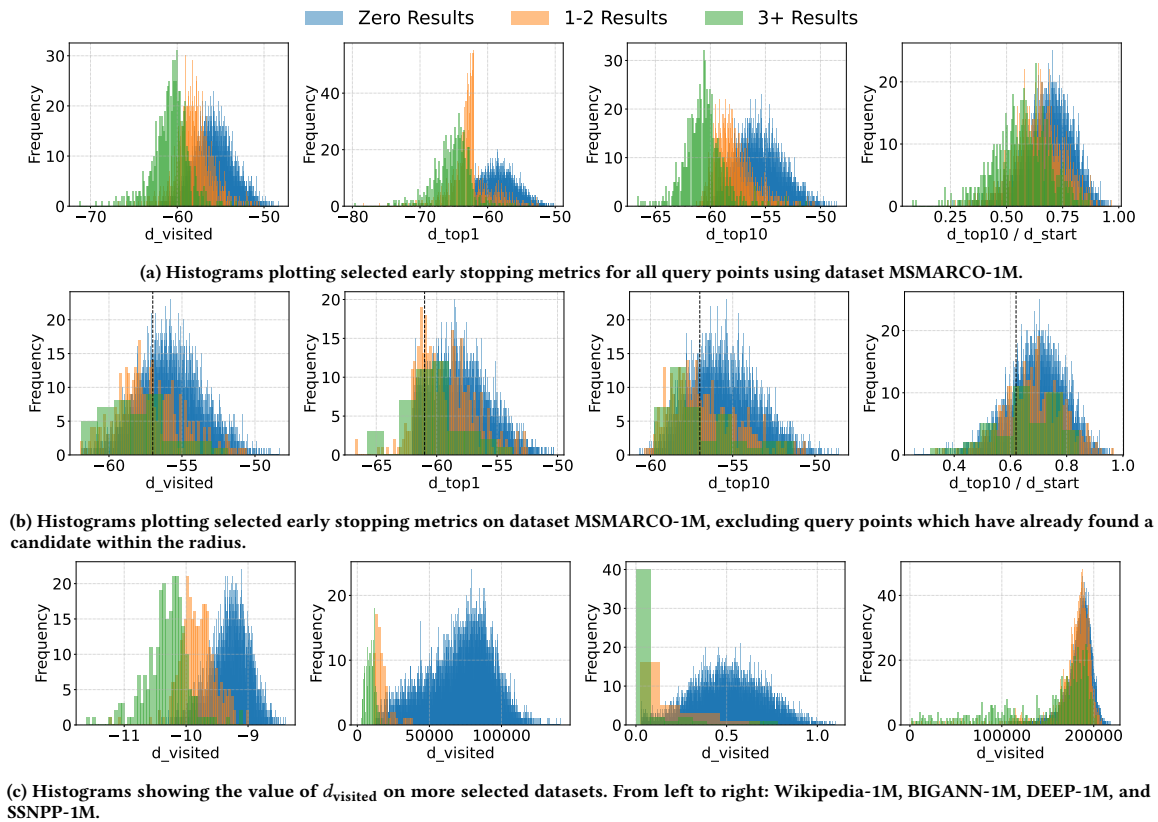


Figure 5: Histograms of early stopping metrics for selected metrics and datasets. All metric values were taken at step 20 of a beam search with beam 100. Queries are separated by color based on the number of range results.

## 5 Experimental Results

In this section, we conduct an experimental evaluation of our algorithms on the nine datasets covered in Section 3. In addition to plotting the QPS and precision tradeoffs for each dataset, we evaluate the time breakdown of each algorithm and draw conclusions about the reasons for their effectiveness.

*Experimental Setup and Code* Our algorithms were implemented as extensions of the ParlayANN [17] library, which is implemented in C++ using ParlayLib [1] for fork-join parallelism as well as standard building blocks such as sorting and filtering. The code will be made available after the anonymous review period. All experiments were conducted on an Azure Standard\_L32s\_v3 virtual machine, with a 3rd Generation Intel® Xeon® Platinum 8370C (Ice Lake) processor in a hyper-threaded configuration. It has 32 vCPUs available to the user and a 256 GB main memory. Experiments use all 32 vCPUs unless otherwise stated.

To produce a curve of QPS versus average precision, the starting beamwidth is varied on a number of searches and the Pareto frontier is reported.

*QPS and Precision Tradeoffs* We begin our experimental evaluation by plotting queries per second (QPS) versus precision for all nine datasets. Data on all datasets except SSNPP can be found in Figure 6; SSNPP is shown in Figure 7, which illustrates the effects of size scaling on the algorithms using datasets SSNPP and BIGANN.

Overall, our algorithms generate improvement over the naive baseline on every dataset, but we find significant diversity in both the magnitude of the improvement and the relative ordering of the two algorithms presented in Section 4. We find that DEEP, BIGANN, and MSTuring experience massive improvement over the baseline (close to 100x improvement in throughput in some cases), with the doubling beam search slightly faster than the greedy search on the 1 million scale, but significantly slower at the 100 million scale. OpenAI also sees large improvement in the realm of one order of magnitude, with greedy search and beam search having virtually identical performance. Wikipedia and MSMarco experience decent improvement with the greedy search somewhat outperforming doubling beam search. GIST achieves such significant improvement over the baseline due to its outlier status with respect to the frequency distribution of its matches, as it is the only dataset with hundreds of points with more than 10000 range results. Greedy search also significantly outperforms doubling beam search for GIST. Text2Image sees modest improvement below 90% recall. SSNPP, which we investigate for three different sizes, first shows little to no improvement at the 1 million scale, then some improvement at the 10 million scale, then significant improvement at size 100 million.

*Scaling* Figure 7 examines the performance of our algorithms on two datasets at three different scales: 1 million, 10 million, and 100 million. Similarly to existing range search benchmarks, we use the

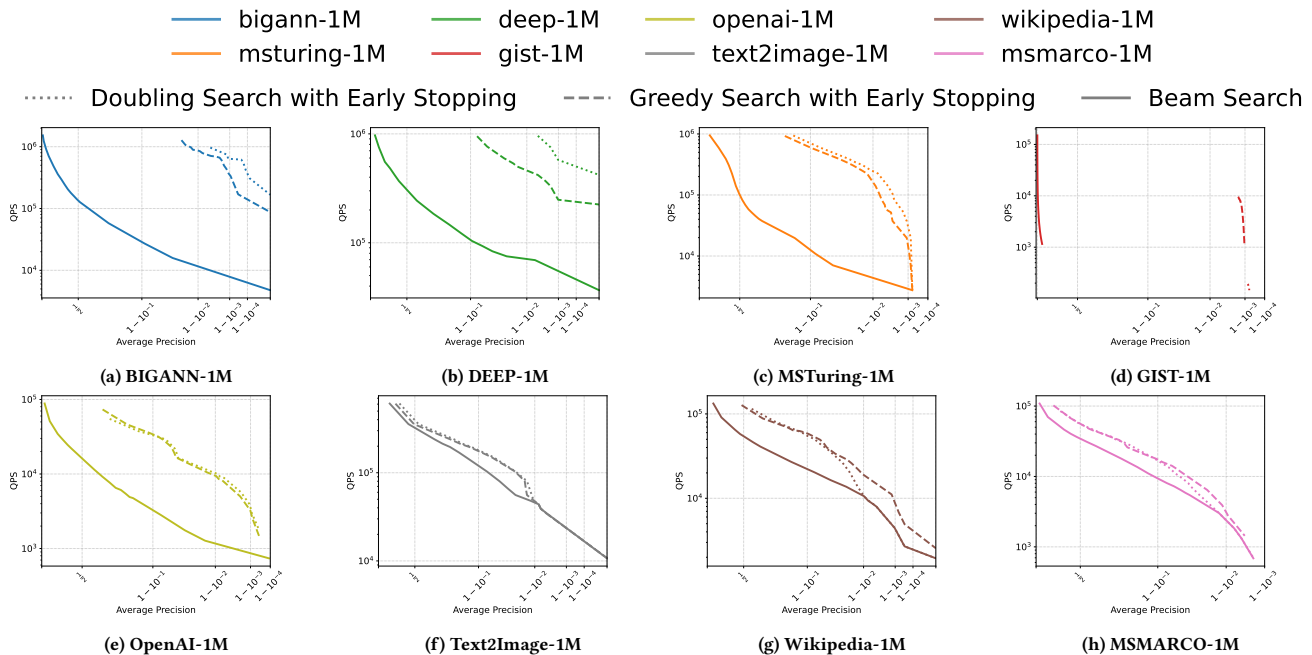


**Figure 6: Average precision vs QPS for eight datasets and three range search algorithms. For GIST-1M, the lines for doubling search and greedy search are very short due to even the smallest of initial beam sizes producing recall in the .999 range.**

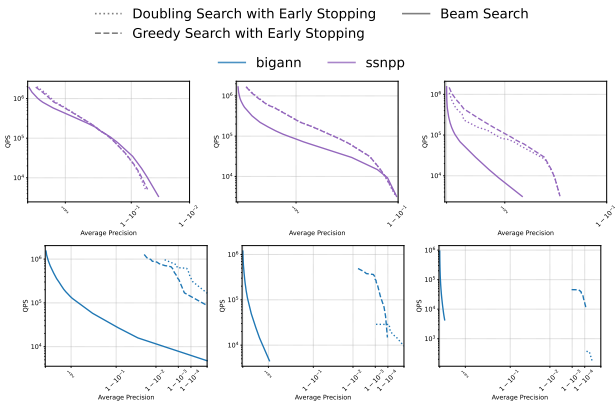


**Figure 7: Average precision vs QPS for the SSNPP and BIGANN datasets. From left to right, slices of size 1 million, 10 million and 100 million.**

same radius for each data scale, so each order of magnitude effectively represents a more dense space, and the average number of results per query point increases. Unsurprisingly, the advantage of our algorithms increases significantly over the baseline, which is only capable of returning up to about 1000 points per query before becoming hopelessly inefficient. Interestingly, we also see that the greedy search seems to have a significant advantage over the doubling beam search as the density of the dataset increases (this is also true of GIST-1M, which has some extraordinarily dense outliers). This is likely because in denser graphs, the greedy search is particularly adept at efficiently finding all points within the radius, which are likely to be in a dense connected cluster in the graph structure. Additional data on size scaling can be found in Appendix A.

*Analyzing Time Spent on Algorithm Components* To aid in our analysis, we investigate the time spent on different phases of each algorithm in Figure 8. Each algorithm consists of an initial beam search phase—either with or without the early stopping criteria in Algorithm 3—and then a following phase of either greedy search or successive calls to doubling beam search. We show this visual breakdown for three datasets at selected fixed average precision: BIGANN-1M, MSMARCO-1M, and GIST-1M.

The time breakdowns provide significant insight into the results in Figures 6 and 7. First, note that for all datasets, the initial beam search phase is a sizable portion of the overall cost of computation. This is because the initial beam search takes place on all points, but further searches only take place on points with one or more valid range result (since the distances used are exact, a point with zero results will never pass on to the second round of computation).

*Greedy Search vs Doubling Search* Next, let us examine the differences between doubling search and greedy search. Doubling search spends a significantly longer portion of time in the second phase of search compared to greedy search, but is capable of achieving higher recall from a smaller starting beam. The characteristics of each individual dataset seem to determine which approach provides the best tradeoff between QPS and average precision. Greedy search requires a larger initial beam to achieve a particular recall value, but the second round of search is extremely cheap as it only visits points within the radius. On the other hand, doubling beam search requires a smaller initial beam, but spends more time in the second phase of search, which performs comparatively more distance comparisons to points which are not valid range results. It also has some overheads related to repeated calls to the beam search function. Based on these factors and the experimental results, it appears that doubling search dominates greedy search when a)

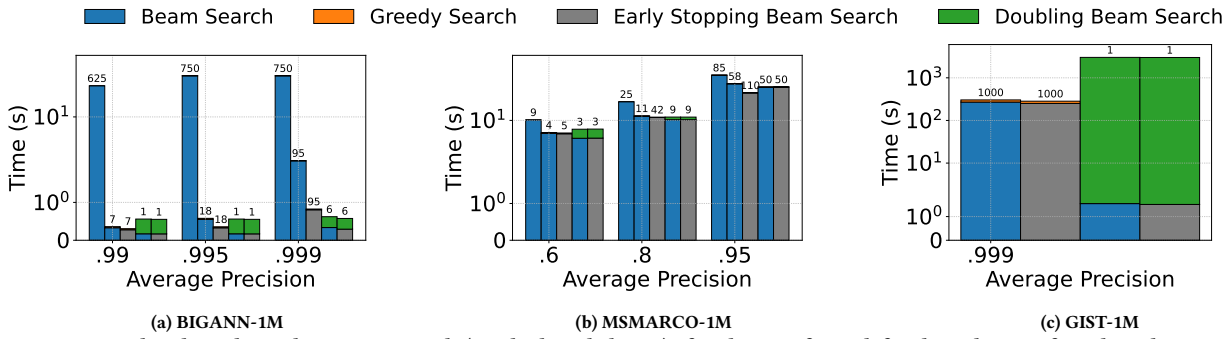


Figure 8: Figures breaking down the cost in seconds (single threaded time) of each type of search for three datasets for selected average precision. The label at the top of each column indicates the beam width of the initial search. Each collection from left to right shows: the beam search baseline, beam search followed by greedy search, beam search with early stopping followed by greedy search, beam search followed by doubling beam search, and beam search with early stopping followed by doubling beam search. Note that in some cases, the time spent on the second phase of search is so short that it is not visible. GIST-1M has only one selected recall, as every search setting yields .999 recall within a .001 tolerance; the beam search baseline is not present for GIST, since it cannot achieve the desired recall (see Figure 6d).

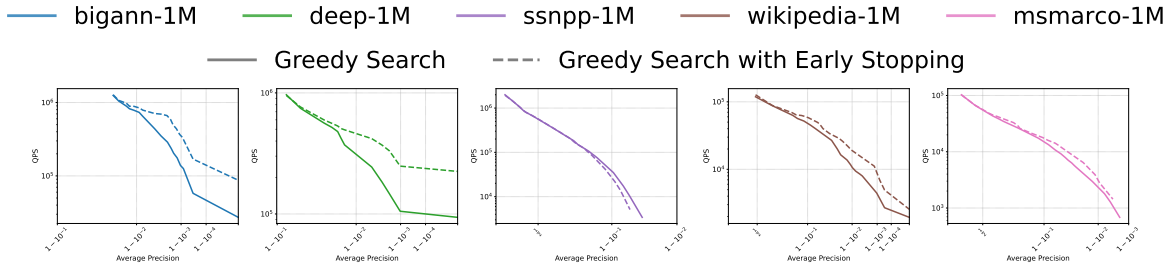


Figure 9: Average precision vs QPS for five selected datasets, showing greedy search without (solid line) and with (dashed line) early stopping.

small initial beam is sufficient for doubling search to achieve high recall, and b) a fairly small number of rounds of doubling search are required. These conditions are met with datasets BIGANN-1M (and DEEP-1M, although its time breakdown is not pictured), but GIST-1M requires too many rounds of doubling, and MSMARCO-1M requires too high an initial beam. We also see that in the scaling studies in Figure 7, the greedy search overtakes the doubling search as the density of matches increases, also likely because many rounds of doubling search become necessary.

*Effects of Early Stopping* Finally, we consider the benefit of early stopping. Early stopping clearly decreases the time taken for a fixed beam; for example, in Figure 8a, early stopping beam search with beam 95 takes less than half the time compared to beam search with beam 95 without early stopping. On the other hand, as illustrated in Figure 8b, early stopping can make the search significantly less accurate due to points with valid range results being terminated too early. The effects of early stopping on selected datasets are shown in Figure 9 and expanded on in Appendix A; overall, early stopping is beneficial on datasets where significant separation exists between the distributions of points with no results and points with one or more results, and not beneficial otherwise.

*Comparison with Top-k Search* We add a final note on comparison with top-k search. To investigate this, we ran top-10 searches on OpenAI-1M and MSTuring-1M, and measured the QPS at 90% 10@10 recall. For OpenAI-1M, we found the QPS at 90% recall was around 5000, compared to around 10000 QPS for range search at 90% precision. For MSTuring-1M, the QPS at 90% recall for top-10

search was about 30000, compared to over 100000 for range search using our algorithms. This suggests that range benchmarking may actually be thought of as an easier problem than top-k search.

## 6 Conclusion

We present a set of algorithms for range retrieval on high-dimensional datasets using graph-based indices. To improve the performance of queries with no range results, we introduce an early stopping mechanism capable of significantly decreasing the time taken to terminate searches on such queries. We also introduce two extensions of beam search, greedy search and doubling search, for efficient range queries with hundreds to tens of thousands of results. Combined, our techniques achieved up to 100x speedup over a naive baseline, with 5-10x speedup in almost all cases. We introduce a benchmark of nine datasets, including datasets with up to 100 million points, and demonstrate strong performance and scalability for our algorithms on these datasets.

Our results yield significant improvement over the naive baseline, and established a wide-ranging benchmark for performance. As we tackle a relatively unexplored problem, many areas for further improvement are still available. One natural extension would be to explore more sophisticated metrics for our early stopping algorithm, perhaps using machine learning methods, as better early termination of queries with few results has potential for significant impact on overall search times. Another would be to explore extensions of the range retrieval benchmark itself; for example, Szilvasy et al. [24] argue that the range search benchmark should differentiate between results which are very close to the query point and points which are close to the radius boundary, giving the for-



mer more weight. In preliminary experiments, we attempted to use a simple weighting mechanism based on a point's distance to the query point when calculating precision, but we were unable to find a weighting that changed the precision values significantly. However, future work identifying such mechanisms would be very practical and promising.

### **Acknowledgments**

This work was supported in part by the National Science Foundation grants CCF-2119352 and CCF-1919223.

## References

- [1] [n. d.]. ParlayLib: A Toolkit for Programming Parallel Algorithms on Shared-Memory Multicore Machines. <https://cmuparlay.github.io/parlaylib/> ([n. d.]).
- [2] Laurent Amsaleg and Herve Jegou. 2010. Datasets for approximate nearest neighbor search. <http://corpus-texmex.irisa.fr/>.
- [3] Dmitry Baranchuk and Artem Babenko. 2021. Deep1B Dataset. <https://research.yandex.com/blog/benchmarks-for-billion-scale-similarity-search>.
- [4] Bernard Chazelle, Ding Liu, and Avner Magen. 2008. Approximate range searching in higher dimension. *Comput. Geom.* 39, 1 (2008), 24–29. <https://doi.org/10.1016/J.COMGEO.2007.05.008>
- [5] Qi Chen, Xiubo Geng, Corby Rosset, Carolyn Buracton, Jingwen Lu, Tao Shen, Kun Zhou, Chenyan Xiong, Yeyun Gong, Paul Bennett, Nick Craswell, Xing Xie, Fan Yang, Bryan Tower, Nikhil Rao, Anlei Dong, Wenqi Jiang, Zheng Liu, Mingqin Li, Chuanjie Liu, Zengzhong Li, Rangan Majumder, Jennifer Neville, Andy Oakley, Knut Magne Risvik, Harsha Vardhan Simhadri, Manik Varma, Yujing Wang, Linjun Yang, Mao Yang, and Ce Zhang. 2024. MS MARCO Web Search: A Large-scale Information-rich Web Dataset with Millions of Real Click Labels. In *Companion Proceedings of the ACM on Web Conference 2024 (WWW '24)*.
- [6] Matthijs Douze, Alexandr Guzhva, Chengqi Deng, Jeff Johnson, Gergely Szilvasy, Pierre-Emmanuel Mazaré, Maria Lomeli, Lucas Hosseini, and Hervé Jégou. 2024. The Faiss library. *CoRR abs/2401.08281* (2024). <https://doi.org/10.48550/ARXIV.2401.08281> arXiv:2401.08281
- [7] Matthijs Douze, Giorgos Tolias, Ed Pizzi, Zoë Papakipos, Lowik Chanussot, Filip Radenovic, Tomáš Jeníček, Maxim Maximov, Laura Leal-Taixé, Ismail Elezi, Ondrej Chum, and Cristian Canton-Ferrer. 2021. The 2021 Image Similarity Dataset and Challenge. *CoRR abs/2106.09672* (2021). arXiv:2106.09672 <https://arxiv.org/abs/2106.09672>
- [8] Cong Fu, Chao Xiang, Changxu Wang, and Deng Cai. 2019. Fast Approximate Nearest Neighbor Search With The Navigating Spreading-out Graph. *Proc. VLDB Endow.* 12, 5 (2019), 461–474. <https://doi.org/10.14778/3303753.3303754>
- [9] Ryan Greene, Ted Sanders, Lilian Weng, and Arvind Neelakantan. 2022. New and improved embedding model. <https://openai.com/index/new-and-improved-embedding-model/>.
- [10] Jonathan Halcrow, Alexandru Mosoi, Sam Ruth, and Bryan Perozzi. 2020. Grale: Designing Networks for Graph Learning. In *SIGKDD Conference on Knowledge Discovery and Data Mining (KDD)*. 2523–2532. <https://doi.org/10.1145/3394486.3403302>
- [11] Piotr Indyk and Rajeev Motwani. 1998. Approximate Nearest Neighbors: Towards Removing the Curse of Dimensionality. In *Proceedings of the Thirtieth Annual ACM Symposium on the Theory of Computing, Dallas, Texas, USA, May 23–26, 1998*, Jeffrey Scott Vitter (Ed.). ACM, 604–613. <https://doi.org/10.1145/276698.276876>
- [12] Herve Jegou, Matthijs Douze, and Cordelia Schmid. 2010. Product quantization for nearest neighbor search. *IEEE Transactions on Pattern Analysis and Machine Intelligence (TPAMI)* 33, 1 (2010).
- [13] Conglong Li, Minjia Zhang, David G. Andersen, and Yuxiong He. 2020. Improving Approximate Nearest Neighbor Search through Learned Adaptive Early Termination. In *Proceedings of the 2020 International Conference on Management of Data, SIGMOD Conference 2020, online conference [Portland, OR, USA], June 14–19, 2020*, David Maier, Rachel Pottinger, AnHai Doan, Wang-Chiew Tan, Abdussalam Alawini, and Hung Q. Ngo (Eds.). ACM, 2539–2554. <https://doi.org/10.1145/3318464.3380600>
- [14] Hao Li, Xiaojie Liu, Tao Li, and Rundong Gan. 2020. A novel density-based clustering algorithm using nearest neighbor graph. *Pattern Recognit.* 102 (2020), 107206. <https://doi.org/10.1016/J.PATCOG.2020.107206>
- [15] Yury Malkov and Dmitry Yashunin. 2018. Efficient and robust approximate nearest neighbor search using hierarchical navigable small world graphs. *IEEE Transactions on Pattern Analysis and Machine Intelligence* 42, 4 (2018).
- [16] Magdalen Dobson Manohar, Zheqi Shen, Guy E. Blelloch, Laxman Dhulipala, Yan Gu, Harsha Vardhan Simhadri, and Yihan Sun. 2024. ParlayANN: Scalable and Deterministic Parallel Graph-Based Approximate Nearest Neighbor Search Algorithms. In *Proceedings of the 29th ACM SIGPLAN Annual Symposium on Principles and Practice of Parallel Programming, PPOPP 2024, Edinburgh, United Kingdom, March 2–6, 2024*, Michel Steuwer, I-Ting Angelina Lee, and Milind Chabbi (Eds.). ACM, 270–285. <https://doi.org/10.1145/3627535.3638475>
- [17] Magdalen Dobson Manohar, Zheqi Shen, Guy E. Blelloch, Laxman Dhulipala, Yan Gu, Harsha Vardhan Simhadri, and Yihan Sun. 2025. ParlayANN. Webpage. Retrieved February 7, 2025 from <https://github.com/cmuparlay/ParlayANN>
- [18] MetaAI. 2020. Using AI to detect COVID-19 misinformation and exploitative content. Webpage. Retrieved January 26, 2022 from <https://ai.facebook.com/blog/using-ai-to-detect-covid-19-misinformation-and-exploitative-content/>
- [19] Nils Reimers. 2022. Datasets: Cohere/wikipedia-22-12-en-embeddings. <https://huggingface.co/datasets/Cohere/wikipedia-22-12-en-embeddings>.
- [20] Florian Schroff, Dmitry Kalenichenko, and James Philbin. 2015. FaceNet: A unified embedding for face recognition and clustering. In *IEEE Conference on Computer Vision and Pattern Recognition, CVPR 2015, Boston, MA, USA, June 7–12, 2015*. IEEE Computer Society, 815–823. <https://doi.org/10.1109/CVPR.2015.7298682>
- [21] Harsha Simhadri, George Williams, Martin Aumüller, Artem Babenko, Dmitry Baranchuk, Qi Chen, Matthijs Douze, Lucas Hosseini, Ravishankar Krishnaswamy, Gopal Srinivasa, Suhas Jayaram Subramanya, and Jingdong Wang. 2021. BigANN Benchmarks: Billion-Scale Approximate Nearest Neighbor Search Challenge. <https://big-ann-benchmarks.com/>.
- [22] Harsha Vardhan Simhadri, George Williams, Martin Aumüller, Matthijs Douze, Artem Babenko, Dmitry Baranchuk, Qi Chen, Lucas Hosseini, Ravishankar Krishnaswamy, Gopal Srinivasa, Suhas Jayaram Subramanya, and Jingdong Wang. 2021. Results of the NeurIPS'21 Challenge on Billion-Scale Approximate Nearest Neighbor Search. In *NeurIPS 2021 Competitions and Demonstrations Track, 6–14 December 2021, Online (Proceedings of Machine Learning Research, Vol. 176)*, Douwe Kiela, Marco Ciccone, and Barbara Caputo (Eds.). PMLR, 177–189. <https://proceedings.mlr.press/v176/simhadri22a.html>
- [23] Suhas Jayaram Subramanya, Devvrit, Harsha Vardhan Simhadri, Ravishankar Krishnaswamy, and Rohan Kadekodi. 2019. Rand-NSG: Fast Accurate Billion-point Nearest Neighbor Search on a Single Node. In *Advances in Neural Information Processing Systems 32: Annual Conference on Neural Information Processing Systems 2019, NeurIPS 2019, December 8–14, 2019, Vancouver, BC, Canada*, Hanna M. Wallach, Hugo Larochelle, Alina Beygelzimer, Florence d'Alché-Buc, Emily B. Fox, and Roman Garnett (Eds.). 13748–13758. <https://proceedings.neurips.cc/paper/2019/hash/09853c7fb1d3f8ee67a61b6bf4a7f8e6-Abstract.html>
- [24] Gergely Szilvasy, Pierre-Emmanuel Mazaré, and Matthijs Douze. 2024. Vector search with small radiuses. *CoRR abs/2403.10746* (2024). <https://doi.org/10.48550/ARXIV.2403.10746> arXiv:2403.10746
- [25] Jie Wang, Jian Lu, Zheng Fang, Tingjian Ge, and Cindy X. Chen. 2013. PL-Tree: An Efficient Indexing Method for High-Dimensional Data. In *Advances in Spatial and Temporal Databases - 13th International Symposium, SSTD 2013, Munich, Germany, August 21–23, 2013. Proceedings (Lecture Notes in Computer Science, Vol. 8098)*, Mario A. Nascimento, Timos K. Sellis, Reynold Cheng, Jörg Sander, Yu Zheng, Hans-Peter Kriegel, Matthias Renz, and Christian Sengstock (Eds.). Springer, 183–200. [https://doi.org/10.1007/978-3-642-40235-7\\_11](https://doi.org/10.1007/978-3-642-40235-7_11)
- [26] Mengzhao Wang, Weizhi Xu, Xiaomeng Yi, Songlin Wu, Zhangyang Peng, Xianguyu Ke, Yunjun Gao, Xiaoliang Xu, Rentong Guo, and Charles Xie. 2024. Starling: An I/O-Efficient Disk-Resident Graph Index Framework for High-Dimensional Vector Similarity Search on Data Segment. *Proc. ACM Manag. Data* 2, 1 (2024), V2mod014:1–V2mod014:27. <https://doi.org/10.1145/3639269>
- [27] Mengzhao Wang, Xiaoliang Xu, Qiang Yue, and Yuxiang Wang. 2021. A Comprehensive Survey and Experimental Comparison of Graph-Based Approximate Nearest Neighbor Search. *Proc. VLDB Endow.* 14, 11 (2021), 1964–1978. <https://doi.org/10.14778/3476249.3476255>
- [28] Xiaoliang Xu, Mengzhao Wang, Yuxiang Wang, and Dingcheng Ma. 2021. Two-stage routing with optimized guided search and greedy algorithm on proximity graph. *Knowl. Based Syst.* 229 (2021), 107305. <https://doi.org/10.1016/J.KNOSYS.2021.107305>
- [29] Hongfei Zhang, Xia Song, Chenyan Xiong, Corby Rosset, Paul N. Bennett, Nick Craswell, and Saurabh Tiwary. 2019. Generic Intent Representation in Web Search. In *Proceedings of the 42nd International ACM SIGIR Conference on Research and Development in Information Retrieval, SIGIR 2019, Paris, France, July 21–25, 2019*, Benjamin Piwowarski, Max Chevalier, Éric Gaussier, Yoelle Maarek, Jian-Yun Nie, and Falk Scholer (Eds.). ACM, 65–74. <https://doi.org/10.1145/3331184.3331198>

## A Additional Data

We provide data on early stopping metrics for four additional datasets in Figures 10, 11, 12, and 13.

In Figure 14 and Figure 15, we examine the impact of early stopping on each dataset at the 1 million scale, measuring improvement over both greedy search and doubling search.

In Figure 16 we present further study on size scaling using the Wikipedia dataset at the 1M and 10M scale.

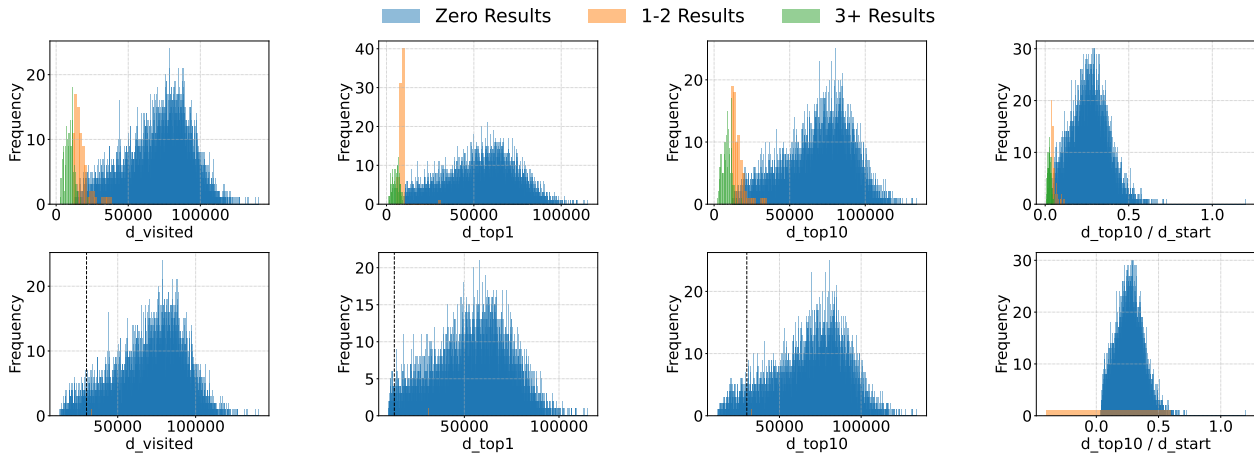


Figure 10: Early stopping metrics for BIGANN-1M, taken at step 20 of a beam search with beam 100. The top row shows all results, while the bottom row shows only results for beam searches that have not yet found a candidate within the radius.

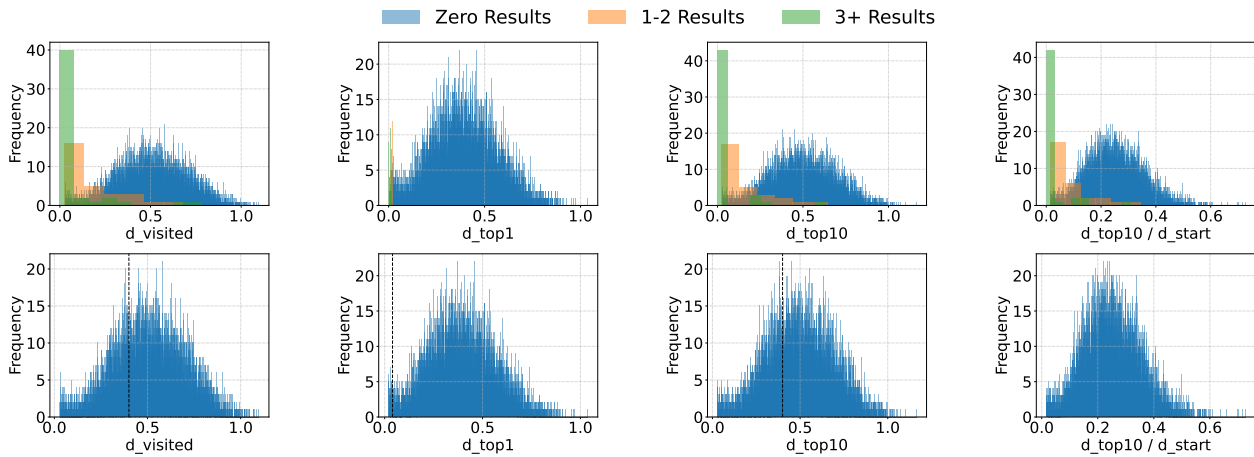


Figure 11: Early stopping metrics for DEEP-1M, taken at step 20 of a beam search with beam 100. The top row shows all results, while the bottom row shows only results for beam searches that have not yet found a candidate within the radius.

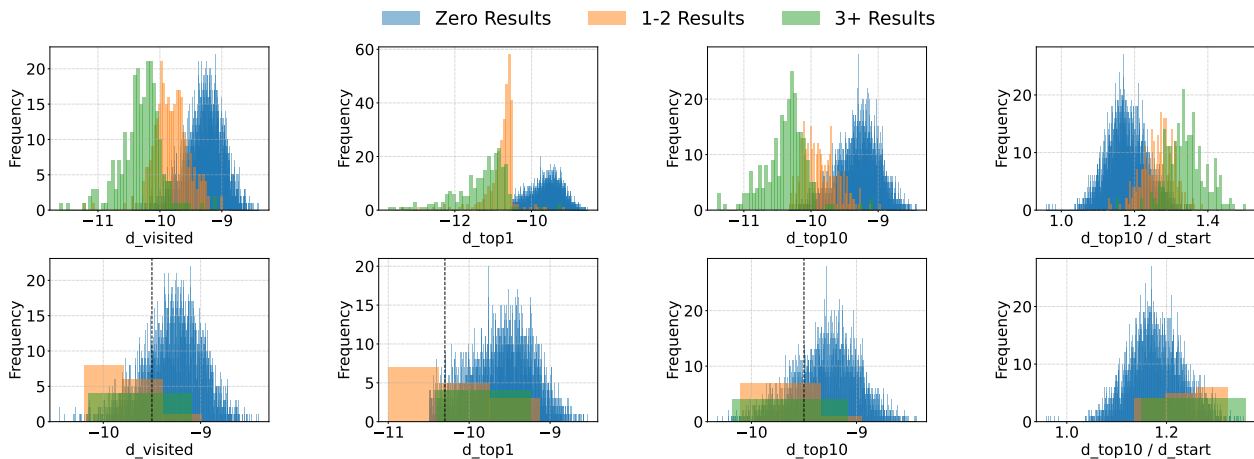
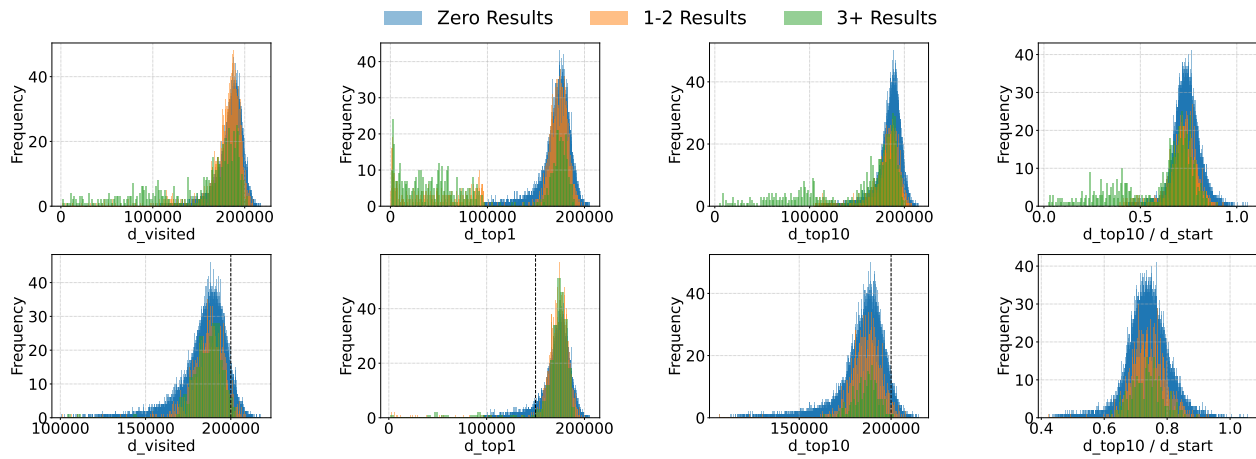


Figure 12: Early stopping metrics for Wikipedia-1M, taken at step 20 of a beam search with beam 100. The top row shows all results, while the bottom row shows only results for beam searches that have not yet found a candidate within the radius.



**Figure 13: Early stopping metrics for SSNPP-1M, taken at step 20 of a beam search with beam 100. The top row shows all results, while the bottom row shows only results for beam searches that have not yet found a candidate within the radius.**

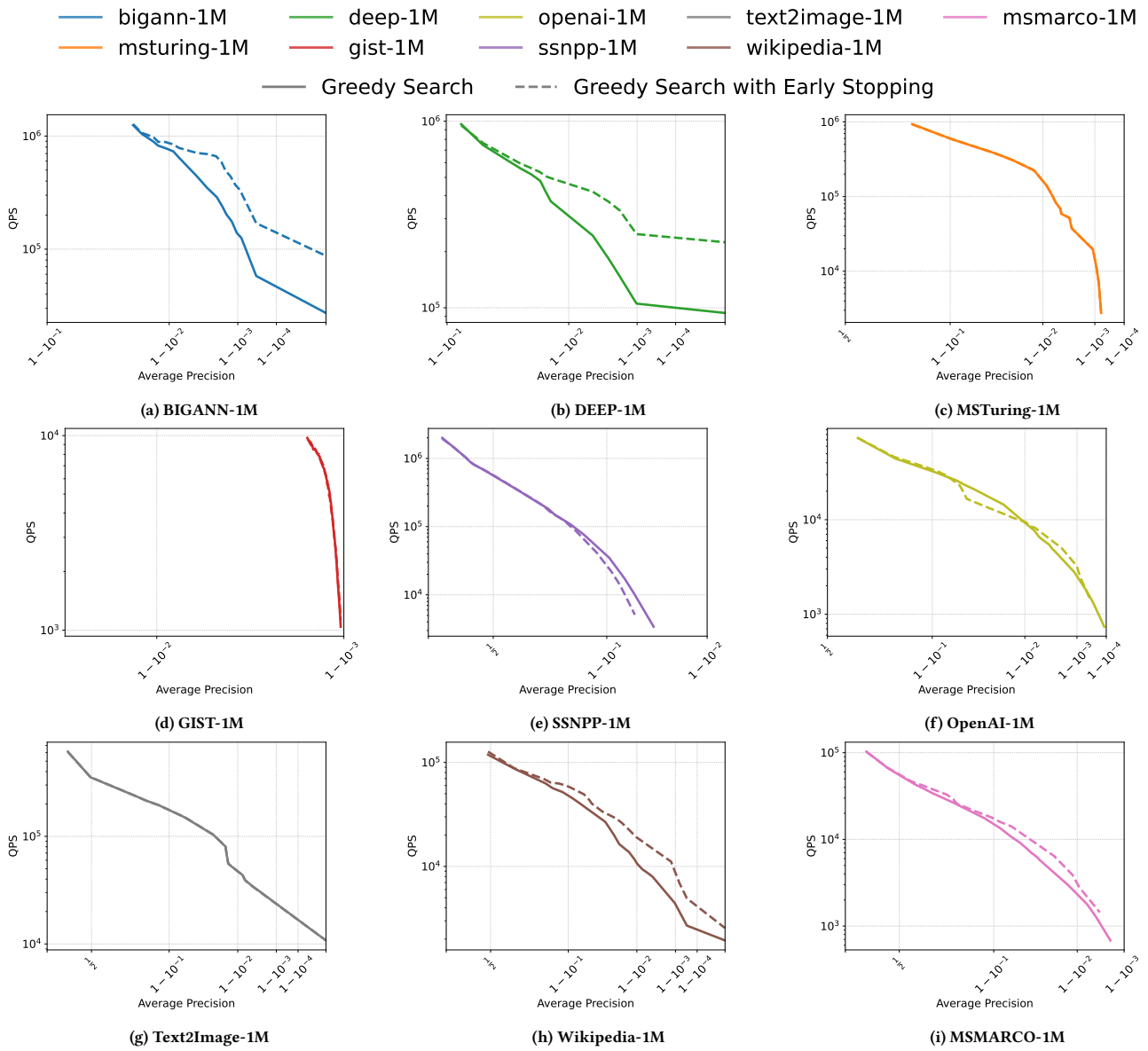


Figure 14: Average precision vs QPS for all nine datasets using greedy search, comparing use of early stopping versus without early stopping.

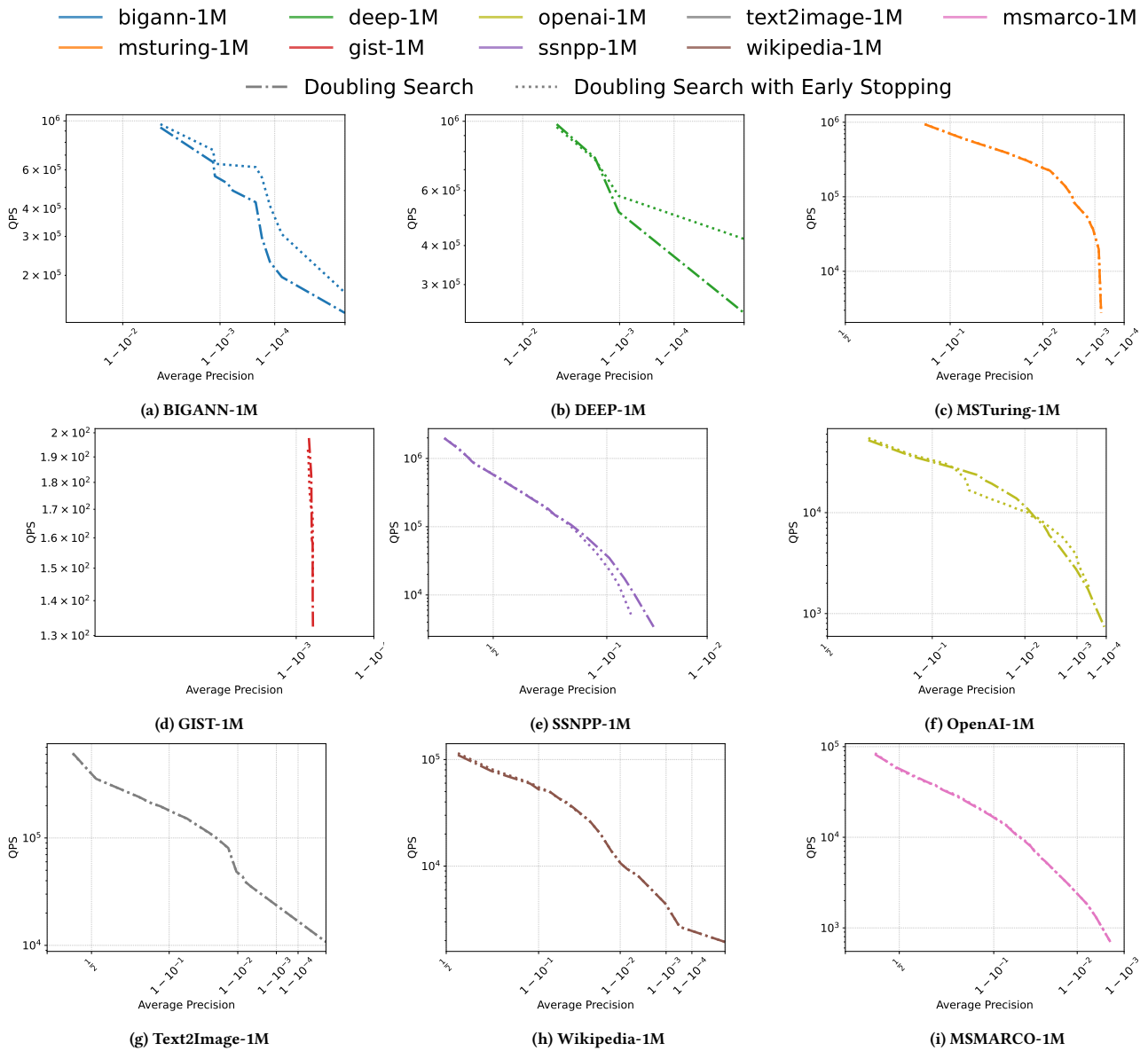


Figure 15: Average precision vs QPS for all nine datasets using doubling search, comparing use of early stopping versus without early stopping.

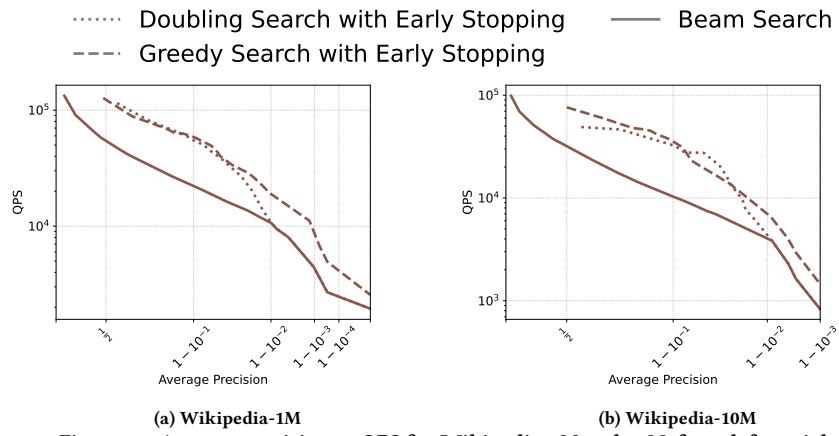


Figure 16: Average precision vs QPS for Wikipedia-1M and 10M, from left to right.